Infrared Quenching and a Unified Description of Photoconductivity Phenomena in Cadmium Sulfide and Selenide

RICHARD H. BUBE
Radio Corporation of America, RCA Laboratories Division, Princeton, New Jersey
(Received April 27, 1955)

Infrared quenching, superlinearity, temperature dependence, and slow S-shape growth of photocurrent in cadmium sulfide and cadmium selenide crystals may all be associated with the filling and emptying of a specific set of defect levels, as indicated by the location of the calculated electron Fermi level. Infrared quenching of photoconductivity occurs only when the Fermi level lies less than 0.8 ev from the conduction band in CdS, or less than 0.6 ev in CdSe; superlinear photoconductivity occurs only when the Fermi level varies between 0.6 and 0.8 ev from the conduction band in CdS, or between 0.3 and 0.6 ev in CdSe; the photosensitivity decreases rapidly as the Fermi level drops further than 0.6 ev from the conduction band in CdS with increasing temperature, or further than 0.3 ev in CdSe; a slow, S-shaped growth of photocurrent is observed when the Fermi level rises between 0.8 and 0.6 ev from the conduction band in CdS, or between 0.6 and 0.3 ev in CdSe.

Infrared quenching maxima for photon energies of 1.65, 1.35, and 0.89 ev are found for CdS, and 1.20, 1.05, and 0.79 ev for CdSe. The magnitudes of the two lower-energy quenching maxima have a constant ratio to one another (as determined from measurements on CdS), as they vary in different crystals, and are most prominent in photosensitive crystals.

INTRODUCTION

ROOM temperature measurements of (1) infrared quenching of photoconductivity and (2) photocurrent as a function of light intensity, for cadmium sulfide and cadmium selenide crystals, lead to an apparent paradox. The concepts of recombination processes advanced by Rose[1] indicate that both infrared quenching and superlinear photoconductivity (i.e., photocurrent increasing with light intensity according to a power greater than unity) should be associated with the filling and emptying of the same set of levels. It is therefore expected either that both phenomena would occur in a given crystal, or that neither phenomenon would occur. Room temperature measurements, however, show that generally CdS crystals show infrared quenching, but not superlinear photoconductivity[2]; crystals of CdSe show superlinear photoconductivity, but not infrared quenching.

It is one of the purposes of this paper to demonstrate that this apparent paradox can be resolved in essential agreement with the general concepts of recombination processes which have been developed. Further data are also provided to aid in correlating these phenomena with the properties of crystal defects.

In brief, it is shown that the superlinear photoconductivity associated with the centers which give rise to infrared quenching in CdS at room temperature, can be detected at elevated temperatures; the infrared quenching associated with the centers which give rise to superlinear photoconductivity in CdSe at room temperature, can be detected at lower temperatures.

Another purpose of this paper is to show that a close correlation exists between infrared quenching, superlinearity, temperature dependence, slow S-shape growth of photocurrent in CdS and CdSe, and the calculated location of the quasi- or steady-state electron Fermi level.[3,4] This Fermi level, E_f, is calculated from the conductivity and the temperature according to the equation

$$E_f = kT \ln(N_c e\mu/\sigma), \tag{1}$$

where T is the absolute temperature, N_c is the concentration of states in the lowest kT-wide part of the conduction band, e is the electronic charge, μ is the mobility (assumed to be 100 cm^2/volt sec),[5] and σ is the conductivity. $\sigma/e\mu$ is simply the concentration of conduction electrons. A similar hole Fermi level can be defined in terms of the concentration of free holes and the concentration of states in the highest kT-wide part of the valence band.

In describing electronic phenomena, it is convenient to consider these Fermi levels as indicating the approximate boundary between shallow trapping centers, lying above the electron Fermi level or below the hole Fermi level, and recombination centers, lying between the two Fermi levels. If a level does not lie between the two Fermi levels, it is assumed that it is in thermal equilibrium with the nearest allowed band, and does not play an appreciable role in recombination processes. The actual boundary between trapping and recombination centers, sometimes called the demarcation level,[6]

[1] A. Rose, Phys, Rev. **97**, 322 (1955).
[2] This paper discusses results obtained principally with "pure" CdS and CdSe crystals. In evaporated or sintered layers of CdS [see S. M. Thomsen and R. H. Bube, Rev. Sci. Instr., **26**, 664 (1955)] with high proportions of Cu [100–1000 parts per million (ppm)], it is possible to observe a superlinear photoconductivity at room temperature, associated with other levels introduced by the Cu. Photoconductivity phenomena in such CdS:Cu layers is very similar in many respects to that found in CdSe "pure" crystals.
[3] A. Rose, RCA Rev. **12**, 362 (1951).
[4] R. H. Bube, J. Chem. Phys. **23**, 18 (1955).
[5] R. W. Smith, RCA Rev. **12**, 350 (1951).
[6] An electron at the electron demarcation level has equal probability of being thermally excited to the conduction band and recombining with a hole in the valence band. A hole at the hole demarcation level has equal probability of being thermally excited

differs from the Fermi level by a factor of kT times the natural logarithm of the ratio of filled recombination centers to empty recombination centers.[1,7] The difference between Fermi level and demarcation level is usually small; in this paper we shall speak of the Fermi level as if it were also the demarcation level. Unless specified otherwise, it is the electron Fermi level which is referred to in this paper.

Two main pieces of experimental evidence have already been advanced to support the validity of the steady-state Fermi level concept as outlined above: (1) the conductivity at which superlinearity sets in or ceases, with increasing light intensity in CdS or CdSe, varies with the operating temperature in such a way as to give constant values of E_f for the setting in or ceasing of superlinearity,[8] and (2) thermally stimulated current curves obtained for different heating rates have varying magnitudes and temperature locations so as to give constant values of E_f for the current maxima.[4] This paper presents a number of other experimental evidences of a similar nature.

The occurrence of infrared quenching of photoconductivity in CdS and ZnS has been reported by several investigators.[9–11] The most detailed investigation of the nature of the phenomenon to date has been reported by Taft and Hebb.[12] They found two quenching bands with maxima at 0.9 and 1.5 ev, which they associated with excitation of trapped holes in two different types of hole trapes. They also reported that it was possible to attribute the dynamic phenomena involved in an observation of rise and decay of quenching to different time constants in the excitation and quenching processes caused by the same wavelength.

Superlinear photoconductivity in CdSe[5,13] has been investigated as a function of temperature.[8] It was found that superlinearity occurred only when the Fermi level varied between 0.3 and 0.6 ev from the conduction band. Similar measurements for CdS[8] showed that superlinearity occurred at elevated temperatures, when the Fermi level varied between 0.6 and 0.8 ev from the conduction band.

According to the hypothesis advanced by Rose,[1] the explanation of superlinearity and infrared quenching of photoconductivity requires the assumption that there are two classes of recombination centers distributed through the forbidden gap. One possible example is that (1) Class II centers have a capture cross section for holes equal to or greater than that of Class I centers; (2) Class II centers have a capture cross section for electrons less than that of Class I centers, once a hole has been captured; and (3) Class II centers lie below the middle of the forbidden gap and are filled with electrons in the dark. Crystal defects that have the capture cross-section properties stipulated can easily be visualized, purely on electrostatic grounds:

Class I centers:

$$\begin{aligned}[V_a^-]^+ + h^+ &\rightarrow [V_a]^{++},\\ [V_a^{--}]^0 + h^+ &\rightarrow [V_a^-]^+.\end{aligned} \tag{2}$$

Class II centers:

$$\begin{aligned}[V_c]^{--} + h^+ &\rightarrow [V_c^+]^-,\\ [V_c^+]^- + h^+ &\rightarrow [V_c^{++}]^0.\end{aligned} \tag{3}$$

V_c represents a cation vacancy and V_a an anion vacancy. The sign inside the bracket represents the number of trapped electrons or holes; the sign outside the bracket represents the effective charge of the defect with respect to the rest of the crystal.

It is assumed further that Class II centers are distributed over a certain definite energy range in the forbidden gap, located so that at high temperatures and/or low excitation intensities (i.e., for Fermi-levels near the center of the gap), Class II centers lie below the hole Fermi level and only Class I centers act as recombination centers. Then an increase in light intensity over the proper range will lower the hole Fermi level (and raise the electron Fermi level), enable some of the Class II centers to act as recombination centers, and hence cause a shift in the recombination traffic from Class I to Class II centers, i.e., most of the holes formed by excitation will be located in Class II centers, and most of the electrons initially in Class II centers will be located in Class I centers. The effect is to increase the lifetime of a free electron and therefore to increase the photosensitivity. As long as the increasing light intensity lowers the hole Fermi level to include more Class II centers, a superlinear photoconductivity will be observed. (These statements rest on the assumption that the concentration of free electrons and holes is much smaller than the concentration of recombination centers.)

When such a crystal is in a "sensitized" state, i.e., when all or most of the Class II centers are acting as recombination centers, infrared quenching can occur by

---

to the valence band and recombining with an electron in the conduction band. A demarcation level must be defined separately for each type of recombination center as characterized by the ratio of capture cross section for electrons to that for holes.

[7] There is a useful relationship between the electron Fermi-level and the hole demarcation level. The hole demarcation level will lie the same distance above the valence band as the electron Fermi-level lies below the conduction band, with a correction equal to kT times the natural logarithm of the ratio of capture cross section for holes to that for electrons (exactly true only if the concentration of levels in the lowest kT-wide part of the conduction band is the same as the concentration of levels in the highest kT-wide part of the valence band). The sign of the correction is such that the hole demarcation level lies further from the valence band than the electron Fermi level lies from the conduction band if the cross section for holes is greater than the cross section for electrons.

[8] R. H. Bube, in *Proceedings of the Conference on Photoconductivity*, Atlantic City, 1954 (John Wiley and Sons Inc., New York, 1955).

[9] A. E. Hardy, Trans. Am. Electrochem. Soc. **87**, 355 (1945).

[10] R. Frerichs, Phys. Rev. **72**, 594 (1947).

[11] H. W. Leverenz, *An Introduction to Luminescence of Solids* (John Wiley and Sons, Inc., New York, 1950), pp. 164, 302–304, 396.

[12] E. A. Taft and M. H. Hebb, J. Opt. Soc. Am. **42**, 249 (1952).

[13] H. J. Dirksen and O. W. Memelink, Appl. Sci. Research **4B**, 205 (1954).

raising electrons, either from the filled band or from low-lying levels, into the Class II centers. Thus the shift in recombination traffic is reversed, and the photosensitivity is decreased.

The experimental results reported in this paper are used to investigate the problem involved in the determination of the actual location of the defect levels which are responsible for the increased sensitivity responsible for such phenomena as superlinearity, infrared quenching, etc. In the example just discussed above, it was assumed that these levels lay near the filled band. Much of the experimental evidence could be interpreted to indicate that these levels might lie near the conduction band. A discussion of these two possibilities is presented later in the paper.

EXPERIMENTAL

Measurements were made in the photoconductivity apparatus previously described,[4] with which the temperature of a crystal can be varied from −196° to 200°C in an atmosphere of helium. Single crystals of cadmium sulfide and cadmium selenide,[14] prepared by S. M. Thomsen and C. J. Busanovich, were used for the measurements, electrical contact being made using melted indium electrodes.[15]

The bias excitation (hereafter called the primary radiation) for the measurements of infrared quenching was obtained from a GE 1493 incandescent lamp, passed through a 5350 A Farrand filter for measurements with CdS, and through a 6920 A Farrand filter for measurements with CdSe.[16] The primary light flux on the crystal used in these experiments lay in the range between 10^{12} and 10^{13} photons/sec. The quenching radiation (hereafter called the secondary radiation) was obtained from a 500-mm Bausch and Lomb monochromator, used to give 50 A resolution. The secondary flux on the crystal was approximately 10^{14} photons/sec. The photocurrent was recorded on a Leeds and Northrup *X-Y* recorder.

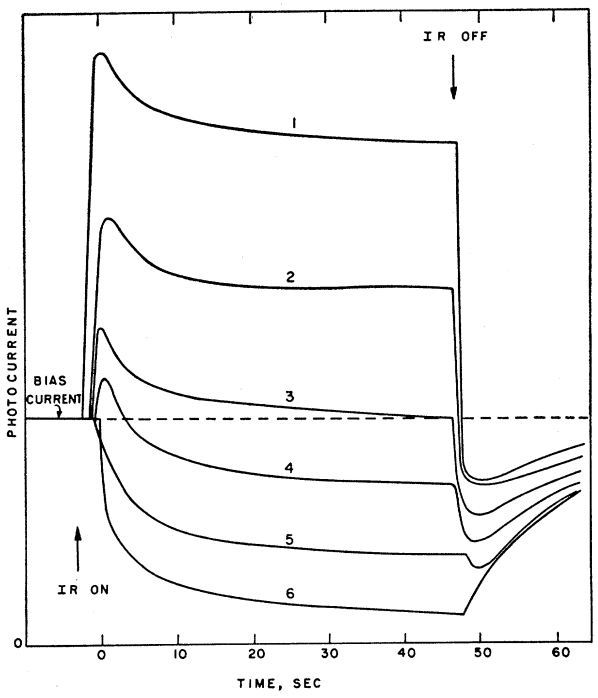

FIG. 1. Dynamic quenching curves for a crystal of CdS for secondary irradiation by wavelengths (1) 6500 A, (2) 6750 A, (3) 7000 A, (4) 7250 A, (5) 7500 A, and (6) 8000 A.

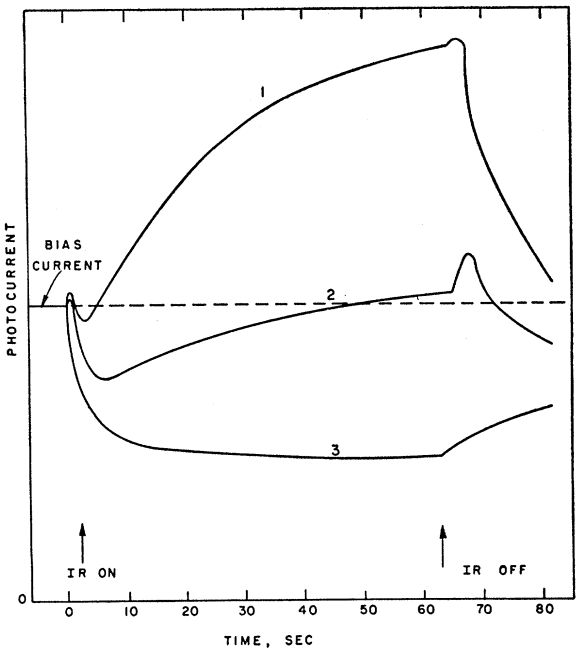

FIG. 2. Dynamic quenching curves for a crystal of CdS for secondary irradiation of wavelengths (1) 7500 A, (2) 7750 A, and (3) 8000 A.

RESULTS

Dynamics of Infrared Quenching

A dynamic method of measurement of infrared quenching was used in this investigation, i.e., the complete curve of photocurrent *vs* time for the onset, equilibrium condition, and end of infrared quenching was recorded for each desired secondary wavelength. Typical results, very similar to those reported by Taft and Hebb,[12] are given in Fig. 1, which is a tracing of actual data obtained for a CdS crystal. The occurrence of a transient maximum current indicates the presence of both excitation and quenching by the secondary radiation. For wavelengths shorter than 6500 A, the current increases asymptotically to an equilibrium value, showing no maximum. As the wavelength of the secondary radiation is increased above 6500 A, the ratio of

[14] R. H. Bube and S. M. Thomsen, J. Chem. Phys. **23**, 15 (1955).
[15] R. W. Smith and A. Rose, Phys. Rev. **92**, 857(A) (1953).
[16] It was established that the quenching spectrum is relatively independent of primary radiation wavelength to a first approximation.

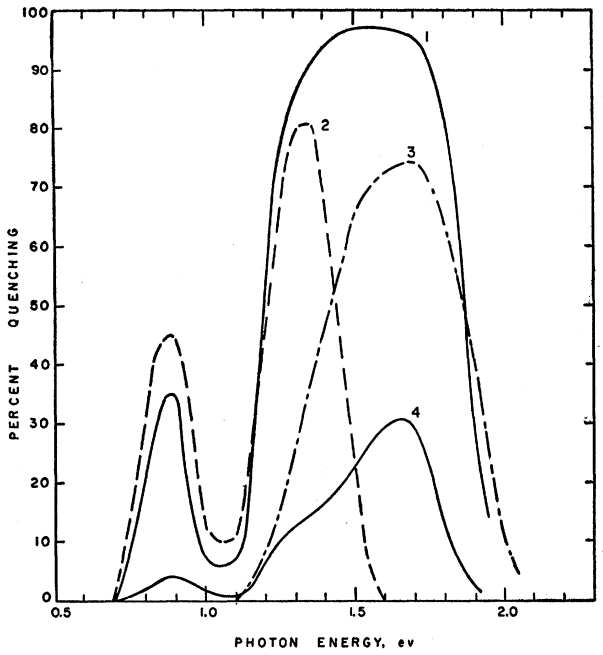

FIG. 3. Infrared quenching spectra at room temperature for four typical crystals of CdS.

excitation to quenching caused by the radiation decreases, until above 7500 A, only quenching remains. Over a broad region of more than a thousand angstroms, however, the secondary radiation causes both excitation and quenching. The form of the curves of Fig. 1 can be explained as was done by Taft and Hebb, by assuming that the excitation caused by the secondary radiation has a higher speed of response than the quenching. When the radiation is removed, the excitation stops very rapidly, but a recovery time is required to remove the quenching effects.

Percent quenching as used in this paper refers to either (1) the ratio of the difference between the equilibrium current and the maximum current, to the maximum current, in cases where the secondary radiation causes some excitation, or (2) the ratio of the difference between the equilibrium current and the bias current, to the bias current, in cases where the secondary radiation does not produce any excitation.

The fact that the form of the dynamic quenching curves can be explained in terms of differing speeds of response for excitation and quenching is dramatically illustrated in Fig. 2. Figure 2 presents a tracing of data obtained for another crystal of CdS, which had a particularly slow excitation speed of response due to trapping effects. Except for the first small increase in current, the curves of Fig. 2 are almost the inverse of the curves of Fig. 1. The curves of Fig. 2 can be explained by assuming that the quenching speed of response of the secondary radiation is higher than the excitation speed of response. The small increase in current found at the turning on of the secondary radiation may be associated with a brief stimulation of electrons from traps.

Infrared Quenching Spectra

It has been previously reported[8] that sensitive CdS crystals show infrared quenching with maximum at about 9000 A, whereas insensitive CdS crystals show quenching with maximum at about 7500 A. These results are explained when it is realized that the main quenching band in CdS consists, not of one band as indicated by Taft and Hebb, but rather of two bands. Figure 3 gives typical infrared quenching spectra for four selected crystals of CdS. Table I summarizes the results obtained with fifteen crystals of CdS, indicating the correlation between the sensitivity of the crystals and the type of infrared quenching spectrum obtained. These measurements were made with constant conductivity produced by the primary radiation. Infrared quenching maxima are found at 0.89 ev and at about 1.35 ev and 1.65 ev.

Some very insensitive crystals of CdS do not show any quenching at all. Insensitive crystal of CdS show predominantly only the 1.65-ev quenching maximum, with half-width of about 0.4 ev. Some relatively insensitive crystals show both the 1.65-ev. and 1.35-ev (half-width of about 0.3 ev) quenching maxima, with about equal magnitudes. The 0.89-ev peak (half-width of about 0.2 ev) occurs when and only when the 1.35-ev peak is found. Sensitive crystals generally show only the 1.35-ev and 0.89-ev quenching maxima. The apparent absence of quenching for photons with energy greater than 1.5 ev in sensitive crystals cannot be taken

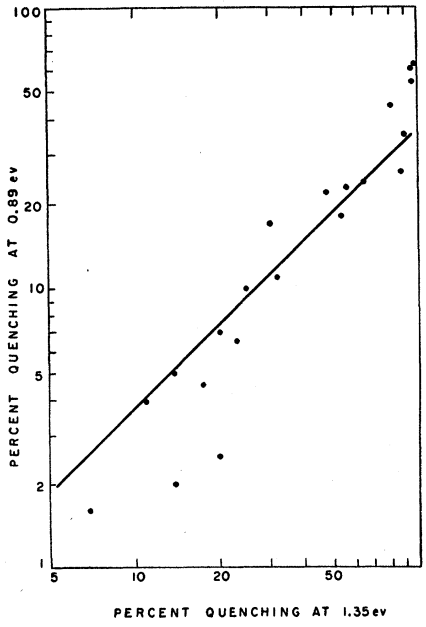

FIG. 4. Percent quenching for photons of 0.89 ev plotted as a function of the percent quenching for photons of 1.35 ev for many different CdS crystals at room temperature.

necessarily as an indication that no quenching occurs in this range. It is possible that the excitation caused by these photons in sensitive crystals overwhelms the quenching effect.[17]

The magnitude of the quenching for the 0.89-ev peak in CdS is plotted as a function of the magnitude of the quenching for the 1.35-ev peak in Fig. 4, for the crystals listed in Table I. Most of the points fall on a straight line with unity slope, indicating a linear relation between the magnitude of quenching, Q, for 0.89-ev and 1.35-ev radiation:

$$Q(0.89 \text{ ev}) = 0.37\, Q(1.35 \text{ ev}). \quad (4)$$

Infrared quenching spectra for three crystals of pure CdSe at −189°C are given in Fig. 5. Three maxima are found for quenching with photons with energies of 1.20, 1.05, and 0.79 ev. Three major differences between quenching in CdS and CdSe are found: (1) CdSe must be cooled in order to obtain measurements of quenching, (2) all crystals of CdSe tested to date have about the same quenching spectrum, and (3) quenching is much stronger in CdSe than in CdS. Since an incandescent source was used to provide the quenching radiation, some correction of the quenching curve for CdSe is required to account for a decrease in the number of photons per second as a function of energy below 0.9 ev. Between 0.9 and 2.0 ev, the output of the monochromator in photons per second as a function of energy is relatively constant. Because of the lack of secondary radiation intensity for photons with energy below 0.9 ev, the possibility of another quenching maxima in this range for CdSe remains, separate from the main quenching band as the maximum at 0.89 ev is separate from the main quenching band in CdS.

TABLE I. Infrared quenching data for CdS crystals.[a]

Crystal type	Relative sensitivity[b]	Percent quenching 0.89 ev	1.35 ev	1.65 ev
A[c]	530	55	96	0
B[d]	175	61	95	33
B	80	11	32	0
C[e]	54	45	81	0
A	12	63	97	99
A	11	22	48	0
B	8.5	5	14	42
C	5.5	17	30	40
A	3.7	2.5	20	81
A	2.2	35	90	97
C	1.2	2	14	80
A	1.0	7	25	76
A	0.80	4	11	31
A	0.53	7	20	35
A	0.19	0	10	75

[a] Measured with a conductivity of 5×10^{-8} mho/cm produced by the primary excitation. Dark conductivity is of the order of 10^{-10} mho/cm.
[b] Sensitivity in microamperes/100 volts for excitation by monochromator at 5150 A.
[c] Type A crystals are "pure" CdS.
[d] Type B crystals are Type A crystals with 10 ppm Al incorporated.
[e] Type C crystals are Type A crystals heated for 5 minutes at 900°C in sulfur vapor and quenched.

[17] In insensitive crystals, excitation is not produced by wavelengths greater than 7500 A. In sensitive crystals, the excitation spectrum may extend as far out as 9000 A.

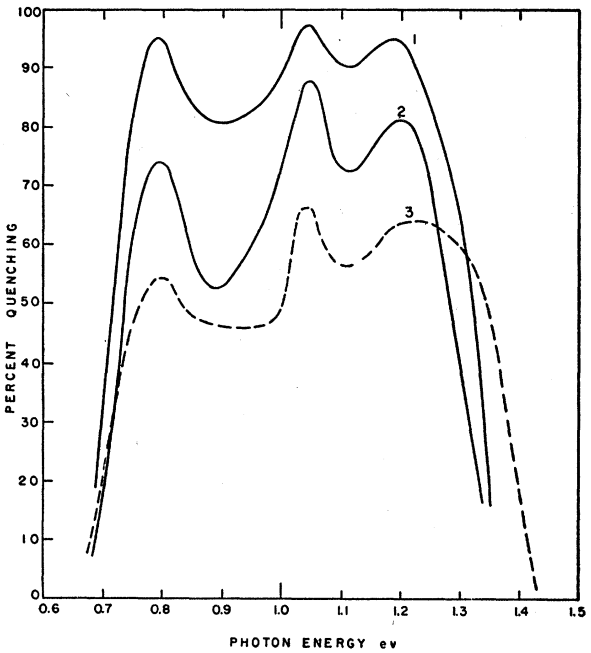

FIG. 5. Infrared quenching spectra at −189°C for three typical crystals of CdSe.

Infrared Quenching as a Function of Intensity

There are two ways to decrease the effective percent quenching: (1) decrease the intensity of the secondary radiation—as illustrated for CdS in Fig. 6(a), and (2) increase the intensity of the primary radiation—as illustrated in Fig. 6(b).

For percent quenching sufficiently far from 100% to avoid saturation effects, the magnitude of the quenching varies approximately linearly (about 0.9 power) with secondary radiation intensity, but varies quite sublinearly (about 0.7 power) with varying primary radiation intensity.

Infrared Quenching as a Function of Temperature

Infrared quenching spectra as a function of temperature, measured at the same conductivity produced by the primary radiation at each temperature, are given in Fig. 7 for a CdS crystal with nearly equal 1.35-ev and 1.65-ev peaks at room temperature, in Fig. 8 for a CdS crystal with larger 1.35-ev peak at room temperature, and in Fig. 9 for a CdS crystal with larger 1.65-ev peak at room temperature. These data show that (1) the 0.89-ev peak vanishes at temperatures below −50°C, (2) at low temperatures all curves shift maximum toward 1.65 ev, even when the room temperature curve shows only a slight quenching at 1.65 ev, (3) all quenching vanishes for temperatures above about 100°C. In analyzing the measurements of infrared quenching as a function of temperature, it must be kept in mind that the intensity of the primary excitation is varied to keep the bias conductivity constant. Insofar

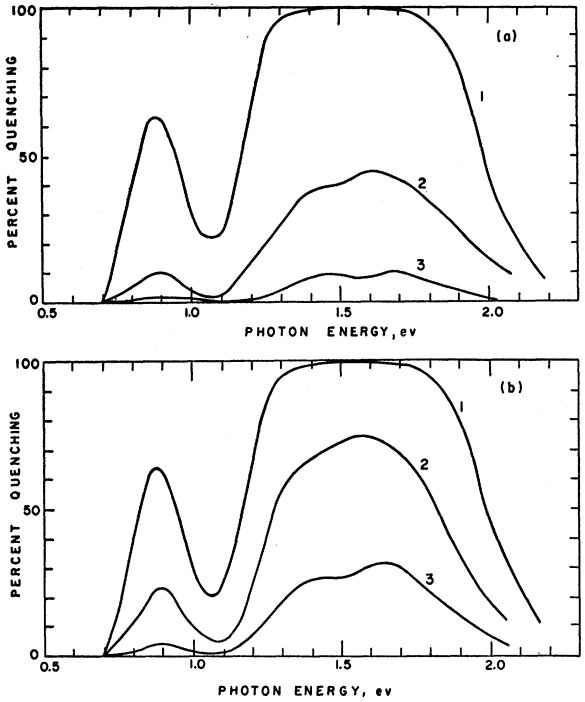

FIG. 6. Infrared quenching spectra at room temperature for a CdS crystal. (a) As a function of secondary radiation intensity: bias current produced by primary excitation of 0.07 μa/100v. (1) Full infrared quenching intensity as used elsewhere in this paper, (2) 14% of full infrared intensity, (3) 2% of full infrared intensity. (b) As a function of primary radiation intensity; secondary radiation intensity same as for (1) in (a). (1) Bias current of 0.07 μa/100v, (2) bias current of 0.36 μa/100v, (3) bias current of 1.8 μa/100v.

as the percent quenching is dependent on the ratio of primary to secondary radiation intensity, some correction for this must be introduced into the interpretation of Figs. 7 through 10. The rather slow variation of percent quenching with primary radiation intensity indicated in Fig. 6(b), however, shows that the major variations of percent quenching with temperature are true temperature effects.

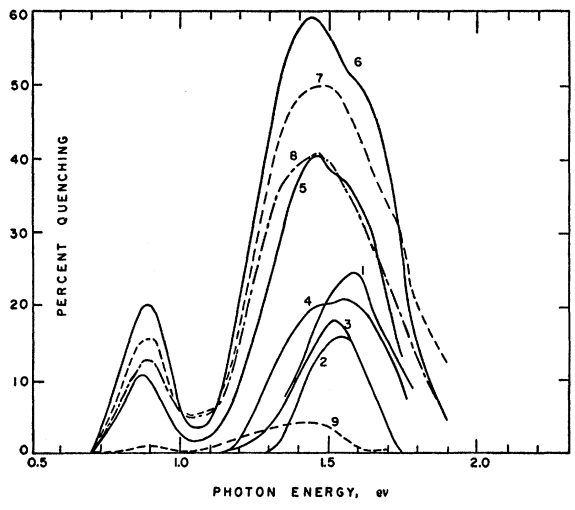

FIG. 7. Infrared quenching spectra for a CdS crystal as a function of temperature in degrees C: (1) −189, (2) −127, (3) −94, (4) −52, (5) −11, (6) 25, (7) 59, (8) 94, and (9) 133.

Figure 10(a) presents data from a more detailed measurement of the temperature variation of quenching by 0.89, 1.35, and 1.65-ev photons in CdS. The inset in Fig. 10(a) shows the temperature variation of the corresponding photocurrent, measured at constant primary light intensity chosen to give a conductivity at room temperature the same as that used for measurements of infrared quenching. All quenching starts to disappear at about the same temperature that the photosensitivity decreases, i.e., about 60°C for the excitation intensity used. Curve 4 in Fig. 10(a) is the relative magnitude of excitation caused by the 1.65 ev secondary radiation,

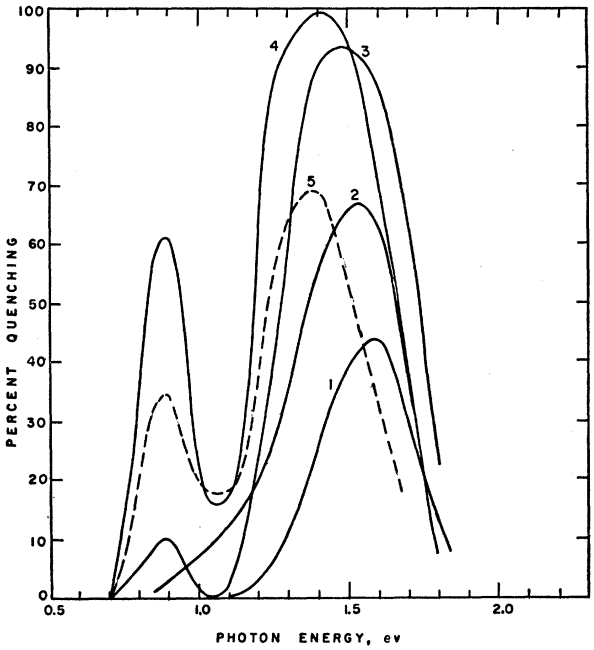

FIG. 8. Infrared quenching spectra for a CdS crystal as a function of temperature in degrees C: (1) −183, (2) −105, (3) −40, (4) 25, and (5) 86.

demonstrating that this is also temperature sensitive; the narrow temperature range over which excitation is observed corresponds to a temperature range where trapping effects are prominent.

Figure 10(b) presents detailed data on the temperature variation of quenching by 1.20, 1.05, and 0.79-ev photons in CdSe. The inset shows the variation of photocurrent at constant primary light intensity. A very rapid decrease in photosensitivity sets in at about −50°C for the excitation intensity used; for higher temperatures the infrared quenching also decreases very rapidly.

The concentration of levels in the neighborhood of the Fermi level may play a large role in determining the

magnitude of the quenching. It is evident that if the Fermi level is so located that the initation of appreciable quenching would cause it to be lowered into a region with a high concentration of filled levels, the subsequent emptying of these levels would serve both to decrease the quenching magnitude and to slow down the establishment of a steady-state condition.

Recovery from Infrared Quenching

The speed of recovery from infrared quenching is increased by the use of a higher primary radiation intensity, and is decreased by the presence of trapping effects. Figure 11 presents curves showing the recovery from infrared quenching (normalized) for two crystals of CdS at room temperature. The shape of the recovery

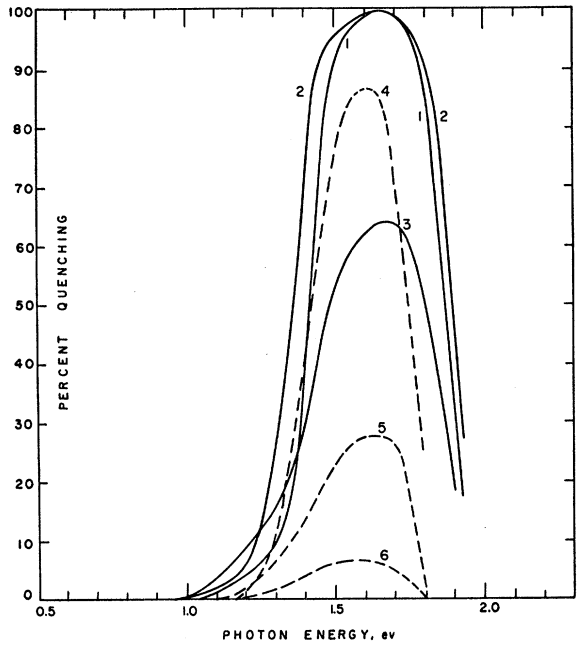

FIG. 9. Infrared quenching spectra for a CdS crystal as a function of temperature in degrees C: (1) −183, (2) −125, (3) −85, (4) −29, (5) 25, and (6) 74.

curves is exponential with time after an initial rapid recovery. There is in most crystals a faster recovery the lower the energy of the quenching photons, relatively independent of the percent quenching which is caused. Sometimes this effect is very marked, as in Fig. 11(a), whereas in other cases, the effect is less obvious although still present, as in Fig. 11(b).

Infrared Quenching and Trapping

The crystals of CdS used in this investigation show a remarkably reproducible trapping distribution from one crystal to another, as determined by measurements of thermally stimulated current. Figure 12 gives the thermally stimulated current curves for four CdS crys-

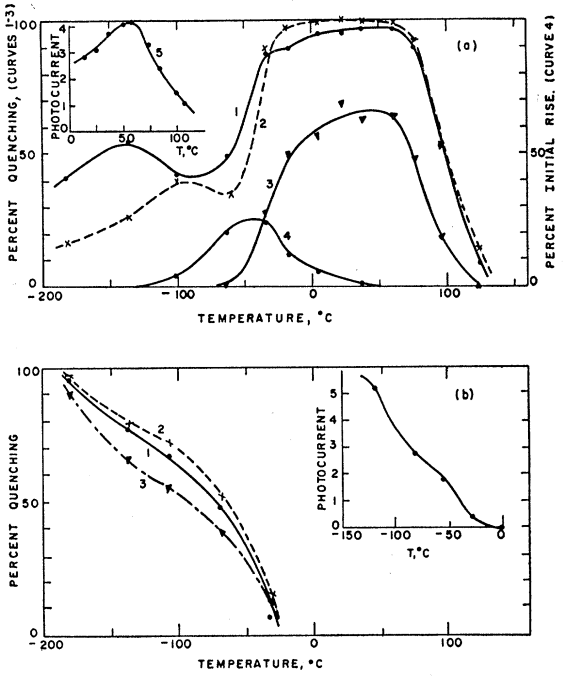

FIG. 10. (a) Temperature variation of percent quenching for a CdS crystal for photons of (1) 1.65 ev, (2) 1.35 ev, and (3) 0.89 ev. Curve (4) is the temperature dependence of the relative magnitude of excitation caused by 1.65-ev radiation. Curve (5) in the inset gives the temperature dependence of the photocurrent at constant primary radiation intensity. (b) Temperature variation of percent quenching for a CdSe crystal for photons of (1) 1.20 ev, (2) 1.05 ev, and (3) 0.79 ev. The curve in the inset gives the temperature dependence of the photocurrent at constant primary radiation intensity.

tals, all of which show evidence of a complex trapping structure involving possibly as many as seven trap depths. The solid curves are for less-sensitive pure CdS crystals, and the dotted curve, the ordinates of which have been multiplied by 0.1 before plotting, is for a sensitive CdS:Al crystal. The shift in the peaks between the dotted curve and the solid curves is exactly that which is required to give the same trap depths (as

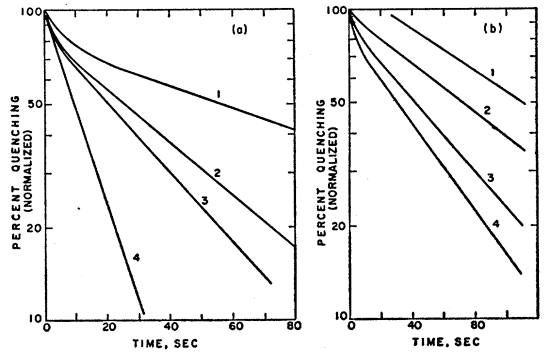

FIG. 11. Recovery from infrared quenching for two CdS crystals: (a) after quenching by radiation of wavelength (1) 7500 or 8000 A, (2) 8500 A, (3) 9000 A, and (4) 9500 A; (b) after quenching by radiation of wavelength (1) 7500 A, (2) 8500 A, (3) 10 000 A, and (4) 14 000 A.

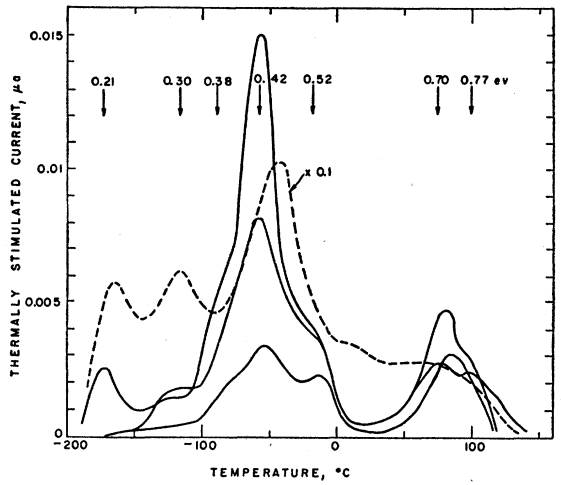

FIG. 12. Thermally stimulated current curves for three "pure" insensitive CdS crystals (solid curves) and a sensitive CdS:Al crystal (dotted curve). Heating rate of 0.77°/sec.

calculated from Fermi levels) for the peak magnitudes and peak temperature locations for all four curves.

In order to determine the effect of infrared quenching on traps, three thermally stimulated current curves were measured, as shown in Fig. 13. A curve run in the normal fashion after 15 minutes in the dark following excitation (Curve 1) is compared with a curve measured after 15 minutes in the dark following excitation, for which the sample was irradiated with 8500 A infrared between −110° and −25°C (Curve 2), and with a curve for which the sample was irradiated with 8500 A infrared for 5 minutes after 10 minutes in the dark following excitation, before the start of the thermally stimulated current measurement (Curve 3).

It must be remembered that the magnitude of the thermally stimulated current at a given temperature depends both on the concentration of traps emptying at that temperature and on the lifetime of a free electron which is dependent on the concurrent distribution of filled and empty states in the forbidden gap. An analysis of the data of Fig. 13 indicates that the decrease in magnitude of the thermally stimulated current found is due completely to a decrease in the free electron lifetime because of the infrared—a decrease which is continuously caused by the infrared in Curve 2, and a decrease which is "built in" by the infrared before the measurement of Curve 3. It is unlikely that the emptying of traps by recombination with free holes is directly related to the mechanism of infrared quenching. In both Curves 2 and 3, there is no decrease in the magnitude of the high-temperature peak, corresponding to levels at a depth of about 0.7 ev.

Infrared Quenching and Photoconductivity Rise Curves

The rise of photoconductivity in CdS crystals at room temperature depends strongly on the length of time which has elapsed since the previous excitation. After periods of darkness of several days, a pronounced *S*-shape rise curve is obtained, more than 20 seconds being required in one case for the photocurrent to rise the first one percent of its equilibrium value.

The same effect on the rise curve can be obtained by irradiating with infrared in the dark before beginning the excitation. In general the rise is slower for those infrared wavelengths which are most effective in quenching the photocurrent caused by a primary excitation.

Figure 14 shows a striking example of the type of rise curve which can be obtained. This measurement was made for a crystal of CdSe at room temperature. (The decrease in the rate of rise by irradiating with infrared in the dark before starting excitation is not found at room temperature for CdSe, but only at lower temperatures.) Figure 14 shows that the rise is initially very rapid, but then changes into a slow *S*-shape rise. The calculated electron Fermi levels for the current at several points are indicated on the curve.

Absorption of Infrared and Excitation

Measurements were made to see if any decrease in infrared transmission through a crystal of CdS could be detected when the crystal was illuminated. With the assistance of H. B. DeVore, a low intensity of infrared was passed through a crystal, which was alternately in darkness and in an intense focused spot of exciting

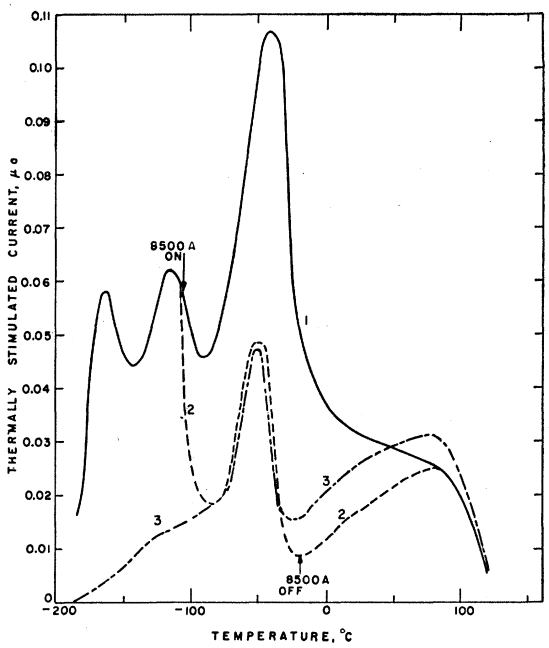

FIG. 13. Thermally stimulated current curves for a CdS crystal: (1) after 15 minutes in dark following excitation; (2) after 15 minutes in dark following excitation, exposed to 8500 A radiation between −110° and −25°C; (3) after 5 minutes exposed to 8500 A ratiation after 10 minutes in the dark following excitation. Heating rate of 0.77°/sec.

radiation. A positive effect, if present, appeared very small: about 1% decrease in transmission for 1.65-ev infrared and about 0.5% decrease in transmission for 1.35-ev infrared.

Fermi-Level Calculations

In order to give an orientation in the discussion which is to follow, Fig. 15 shows how the Fermi level varies with temperature for certain values of conductivity, given on the figure in units of mho/cm$\times 10^{-6}$. For most of the crystals tested for infrared quenching, the geometrical dimensions were such that the conductivity was numerically equal to the current for an applied voltage of 100 volts. Therefore the numbers on the curves of Fig. 15 can be interpreted approximately as the microamps of current for an applied voltage of 100 volts.

DISCUSSION

The phenomena of infrared quenching, superlinearity, temperature dependence, and slow S-shape growth of photocurrent in CdS and CdSe can all be correlated with the location of the calculated electron Fermi level, and hence by inference with the filling and emptying of a certain set of levels in the forbidden gap.

The main features of the following discussion, which sets forth the details of this correlation, are summarized in Table II. Important quantities to be kept in mind are the band gaps of CdS (2.4 ev) and of CdSe (1.7 ev), and the distance between the Fermi level and the conduction band in the dark at room temperature for the conductivity of the crystals used (about 0.8 ev).

Superlinear Photoconductivity

It has previously been shown[8] that superlinear photoconductivity occurs when and only when the Fermi level varies between 0.6 and 0.8 ev from the conduction band in CdS, and between 0.3 and 0.6 ev from the conduction band in CdSe.

Thermally Stimulated Current

It has also been previously shown[8] that every crystal of CdS shows a characteristic thermally stimulated current peak at 0.7 ev, and that every crystal of CdSe shows such a peak at about 0.4 ev.

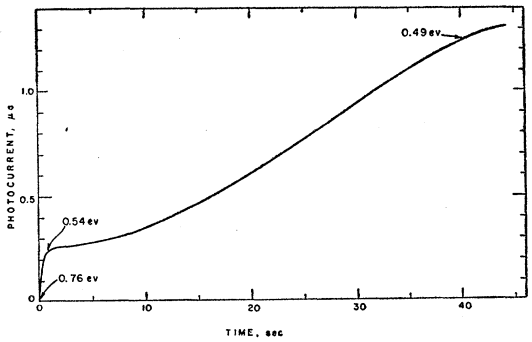

FIG. 14. Growth of photocurrent with time for a crystal of CdSe at room temperature.

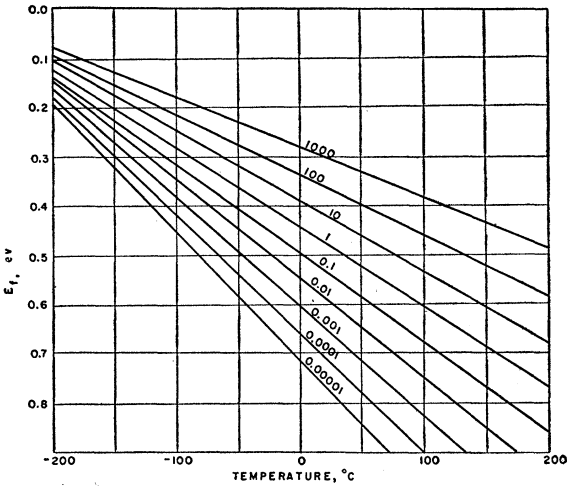

FIG. 15. Calculated distance of the electron Fermi-level from the conduction band as a function of temperature for several values of conductivity in units of mho/cm$\times 10^{-6}$.

Temperature Dependence of Photoconductivity

The photosensitivity of CdS crystals decreases very rapidly when the temperature is raised above that temperature for which the Fermi level is approximately 0.6 ev from the conduction band. The actual temperature breakpoint for photosensitivity is very sensitive to the excitation intensity, lying at lower temperatures for lower excitation intensities in such a way as to give a constant location of the Fermi level for the breakpoint. Similarly the photosensitivity of CdSe crystals decreases very rapidly when the Fermi level drops further than 0.3 ev from the conduction band with increasing temperature.[8] Because of the difference in the critical Fermi level for the two types of crystals, the breakpoint for CdS lies about 100° higher than that for CdSe.

In making many measurements with different pure CdSe crystals, occasionally a crystal is found with very low sensitivity, which has a sublinear variation of photocurrent with light intensity at room temperature instead of a superlinear variation. The correlation between the occurrence of superlinearity and the temperature dependence of photosensitivity is dramatically illustrated by the fact that the photosensitivity of such crystals is practically constant between 25° and 100°C.

Occurrence of Infrared Quenching

The magnitude of infrared quenching has a temperature dependence which is very similar to that of the photosensitivity itself. When the Fermi level drops further than 0.6 ev from the conduction band in CdS, or further than 0.3 ev in CdSe, the magnitude of the quenching decreased very rapidly; no quenching is

TABLE II. Correlation between electronic phenomena in CdS and CdSe and the location of the electron Fermi level, E_f (measured from the conduction band).

	CdS	CdSe
Width of the forbidden gap	2.4 ev	1.7 ev
At room temperature in the dark	$E_f \sim 0.8$ ev	$E_f \sim 0.8$ ev
Superlinear photoconductivity when and only when	0.6 ev $< E_f <$ 0.8 ev	0.3 ev $< E_f <$ 0.6 ev
Thermally stimulated current always shows peak at	$E_f \sim 0.7$ ev	$E_f \sim 0.4$ ev
Temperature quenching of photoconductivity sets in when	$E_f > 0.6$ ev	$E_f > 0.3$ ev
Temperature quenching of the phenomenon of infrared quenching of photoconductivity sets in when	$E_f > 0.6$ ev	$E_f > 0.3$ ev
Infrared quenching peaks at	1.65 ev 1.35 ev 0.89 ev	1.20 ev 1.05 ev 0.79 ev
Slow S-shape of photocurrent when and only when	0.6 ev $< E_f <$ 0.8 ev	0.3 ev $< E_f <$ 0.6 ev

found when the Fermi level lies further than 0.8 ev from the conduction band in CdS, or further than 0.6 ev in CdSe.

Growth of Photocurrent

Slow S-shape growth curves occur only when the Fermi level passes through that portion of the forbidden gap which is between 0.6 and 0.8 ev from the conduction band in CdS, and between 0.3 and 0.6 ev from the conduction band in CdSe. The slow growth corresponds to the time required for readjustment of empty and filled levels in the forbidden gap, holes becoming located at centers with small recombination cross section, and electrons becoming located at centers with large recombination cross section. In the case illustrated in Fig. 14, the growth is rapid as the Fermi level rises from 0.76 to 0.54 ev from the conduction band, but is then very slow as a large increase in sensitivity is caused by readjustment of empty and filled levels in the forbidden gap.

There are two simple models which are suggested by the above data. The following discussion points out the successes and difficulties of each model in accounting for the experimental results.

(1) The characteristic defect levels responsible for the phenomena of superlinearity, infrared quenching, etc. (Class II levels) lie near the conduction band.

The close correlation found in all the cases discussed above between the location of the calculated electron Fermi level and the occurrence of these photoconductivity phenomena suggest directly that the defect levels themselves are located at the distances from the conduction band indicated by the Fermi level.

The occurrence of characteristic thermally stimulated current peaks, indicating the existence of levels at these same distances from the conduction band, suggests that the current peaks are associated with the thermal emptying of the defect levels.

The quenching maxima which occur in all crystals are associated with 1.65-ev photons in CdS and 1.20-ev photons in CdSe. Assuming that these correspond to transitions from the top of the filled band (or from levels near the top of the filled band) to levels higher in the forbidden gap, the distance of these levels from the conduction band is found to be about 0.75 ev in CdS and 0.50 ev in CdSe. Thus these levels are identified with the characteristic defect levels responsible for the various effects previously described. Figure 16(a) indicates the infrared quenching transitions involved in the first model.

The 1.35-ev and 0.89-ev quenching maxima in CdS are closely related and occur prominently only in the more sensitive crystals. Although they have about the same high-temperature breakpoint as the 1.65-ev maximum, it seems probable that they are associated with a different set of defects, the presence of which by itself increases the sensitivity of the crystal by providing centers with small recombination cross section. If these defects were to have two levels associated with them, separated by 0.89 ev, the higher one lying at 1.35 ev from the filled band, then an activation energy of some 0.46 ev would be required to free a hole from the lower level, thus making it available for capture by a center with large recombination cross section. Such an activation energy would agree well with the failure to obtain quenching for 0.89-ev photons below -50°C. Such a mechanism is very similar to that proposed by Taft and Hebb.

It is interesting to note that, on the basis of studies of conductivity in CdS crystals, Kroeger[18] has concluded that the probable height of the level for an anion

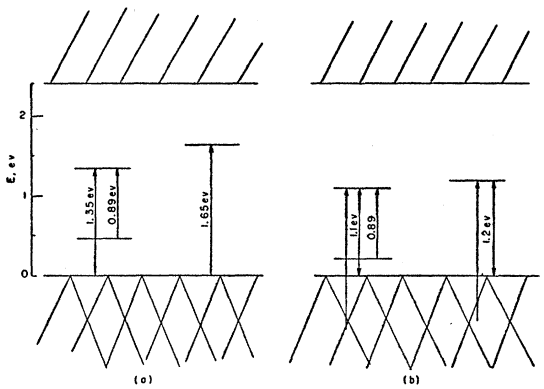

FIG. 16. (a) Infrared quenching transitions for the first model in which the location of the characteristic defect levels is associated with the location of the electron Fermi level; (b) infrared quenching transitions for the second model in which the location of the characteristic defect levels is associated with the location of the hole demarcation level.

[18] Kroeger, Vink, and van den Boomgaard, Z. physik. Chem. **203**, 1 (1954).

vacancy with one trapped electron (hence a Class I center) is about 1.8 ev above the filled band, and that the probable height of the level for a cation vacancy with one trapped hole (hence a Class II center) is about 1.3 ev above the filled band.

The most obvious failure of the model which places the characteristic defect levels near the conduction band, however, is that the simple filling and emptying of levels, lying above the Fermi level and hence empty in the dark, cannot by itself supply the phenomena of superlinearity, infrared quenching, etc., which are observed. Only the measurements of thermally stimulated current fit this model completely. As outlined in the Introduction, it is necessary for the Class II centers to be able to transfer electrons (via the conduction and valence bands) to Class I centers in the process of "sensitization" of the crystal. In the "sensitized" condition, most of the holes are located in small capture cross section Class II centers, and most of the electrons are located in large capture cross section Class I centers, thus giving few large capture cross section centers available for capturing electrons. It is clear that centers empty in the dark do not have associated with them electrons which they can transfer to Class I centers to provide this "sensitization" process.

In this model, with the defect levels located near the conduction band, the only way to obtain the phenomena of superlinearity, infrared quenching, etc. would be to have these phenomena associated with an unidentified type of levels lower in the forbidden gap, which are coupled directly with the high-lying defect levels in such a way that the occupancy of the lower levels depends on the occupancy of the upper levels.

(2) The characteristic defect levels responsible for the phenomena of superlinearity, infrared quenching etc., lie near the filled band.

This assumption is the same as was made in the Introduction and it is therefore clear that levels so located could in principle give rise to the observed phenomena.

If this model were to be adopted, it would be the location of the corresponding hole Fermi level which would be significant, instead of the actual location of the electron Fermi level. To be more precise, it would be the hole demarcation level which would be significant; we have previously pointed out the correlation between the locations of the electron Fermi level and the hole demarcation level. It would be necessary to assume that the hole demarcation level is traversing that portion of the gap near the filled band where the defect levels (Class II) are located, whenever the electron Fermi level is traversing that portion of the gap between 0.6 and 0.8 ev from the conduction band in CdS, and between 0.3 and 0.6 ev from the conduction band in CdSe. In other words, the location of the electron Fermi level is just an indication of the location of the hole demarcation level, and not of the actual location of the Class II defect levels. Since the distance of the hole demarcation level above the filled band is equal to that of the electron Fermi level below the conduction band plus a correction term depending on the ratio of the capture cross sections of the centers for holes and electrons, the exact location of the hole demarcation level requires a knowledge of this cross-section ratio. Since the capture cross section of Class II centers for holes may be as much as a million times or more as large as their capture cross section for electrons, a simple calculation shows that at room temperature the hole demarcation level will lie possibly as much as 0.3 ev further from the valence band than the electron Fermi level lies from the conduction band. When the electron Fermi level varies between 0.6 and 0.8 ev below the conduction band in CdS, therefore, the hole demarcation level is varying approximately between 0.9 and 1.1 ev above the valence band.

On the basis of this model, it must be assumed in addition that the correspondence between the thermally stimulated current peak at 0.7 ev in CdS and 0.4 ev in CdSe with the range of electron Fermi levels associated with the photoconductivity phenomena, is merely a coincidence.

Special consideration must be given the data on infrared quenching from the viewpoint of this model. Taking CdS as an example, it is found that infrared quenching bands with maxima at 1.35 ev and 1.65 ev are found. Transitions of such a large energy can be found only from low-lying levels to the conduction band, or from the filled band or low-lying levels to high-lying levels. The former transition cannot result in quenching, and may be neglected. If the data are considered evidence for actual quenching *bands* with fairly small half-width, transitions from levels near the top of the filled band to levels above the middle of the gap would be indicated, as assumed in the first model discussed above.

It is possible, however, to assume that the "band-shape" of the high-photon-energy quenching spectrum is not intrinsic to the quenching process, but is really caused by a competition between excitation and quenching by high-energy photons, excitation becoming much more prominent with increasing photon energy. On this basis, it might be argued that the significant energy in the quenching spectrum is not the energy for maximum quenching, but the lowest photon energy which will give any quenching at all. This lowest energy represents a threshold energy (the actual distance of the Class II defect levels above the filled band); for photons of higher energy than the threshold energy, the quenching arises from transitions from lower in the valence band, and is large and relatively constant. The average value for this threshold energy obtainable for the quenching data at high photon energies for CdS is about 1.1 or 1.2 ev. The most insensitive crystal, and hence the crystal with the largest value for this minimum energy, has a threshold of approximately 1.2 ev. This value does not differ too much from the estimated

possible location of the hole demarcation level for the occurrence of superlinearity, infrared quenching, etc. It would still seem likely that the 0.89-ev transition must be attributed to a transition from a level near the top of the filled band to the defect levels; in this case the level from which the 0.89-ev transition is made would be located about 0.2–0.3 ev above the filled band. Figure 16(b) indicates the infrared quenching transitions involved in this model.

The author is indebted to Dr. A. Rose, Dr. H. S. Sommers, and M. A. Lampert for many helpful discussions.

PHYSICAL REVIEW VOLUME 99, NUMBER 4 AUGUST 15, 1955

Frequency Dependence of Magnetic Resonance in α-Fe_2O_3

HIROO KUMAGAI, HIDETARO ABE, KAZUO ÔNO, IZUO HAYASHI, JUNJI SHIMADA, AND KENZO IWANAGA
Institute of Science and Technology, University of Tokyo, Tokyo, Japan

(Received April 12, 1955)

Magnetic resonance absorption in single crystals of natural α-Fe_2O_3 was examined in the wavelength range from 5.4 mm to 6.2 cm. Resonance fields H_r observed in the basal plane do not give a quadratic relation with the normal resonance field H_0 as predicted by the usual Kittel formula, but rather the following linear relationship: $h\nu/g\beta = H_0 = H_r + H_A$, where H_A is 4.2_5K oe and g is 2.5_4.

1. INTRODUCTION

MAGNETIC resonance in single crystals of α-Fe_2O_3 has been observed at 1.25-cm wavelength by Anderson *et al.*[1] We refer to their paper as (A) in the following. They assumed the usual Kittel formula[2]:

$$H_0 = [H_r(H_A + H_r)]^{\frac{1}{2}}, \quad (1)$$

where H_0 is the normal resonance field, H_r the observed resonance field in the basal plane, and H_A the anisotropy field in the direction of the ternary axis. Then, under the assumption $g=2$, they obtained the anisotropy field $H_A \simeq 30\,000$ oe. These resonance absorptions may be caused by the parasitic ferromagnetism of this crystal.

We have examined single crystals of natural α-Fe_2O_3 (α-hematite) by the usual method of magnetic resonance absorption at seven different wavelengths (from 5.4 mm to 6.23 cm). The resonances were observed at various orientations of static magnetic field and at room temperature except where the temperature is shown.

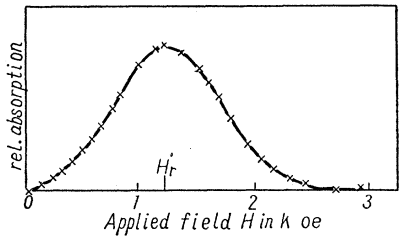

FIG. 1. Resonance absorption in α-Fe_2O_3 at $\lambda = 15.3$ mm and at room temperature. The static magnetic field is applied in the basal plane, i.e., perpendicular to the ternary axis.

[1] Anderson, Merritt, Remeika, and Yager, Phys. Rev. **93**, 717 (1954).
[2] C. Kittel, Phys. Rev. **73**, 155 (1948).

2. EXPERIMENTAL

The samples used were obtained from Sagashima, in the western part of Japan. The crystals have metallic luster and are disk-shaped with a diameter of about 10 mm and a thickness of 0.5–1 mm. They have (magnetically) hexagonal symmetry. The symmetry axis is perpendicular to the disk plane, so we call this the "basal plane." They easily cleave in this plane. Since the absorption is very strong and the nonmagnetic loss is fairly large, thin specimens of about 5-mm^2 area were used. At shorter wavelengths, specimens of only about 0.5-mm^2 area were used.

The method of measurement is almost the same as described elsewhere,[3,4] but in the present case it differs from the past descriptions in two respects. One is that the field modulation method was used to obtain line widths, though the direct galvanometer method was also used at some wavelengths. The other is that we omitted the procedure of tuning the sample cavity to cancel out the dispersion effect accompanied by reso-

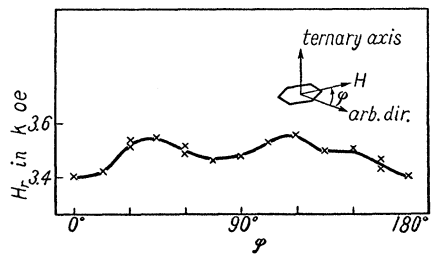

FIG. 2. Variation of resonance field H_r in the basal plane. ($\lambda = 11$ mm.)

[3] H. Kumagai *et al.*, J. Phys. Soc. Japan **9**, 369 (1954).
[4] H. Abe *et al.*, J. Phys. Soc. Japan **9**, 814 (1954).